

Hydrothermal formation of tobermorite studied by *in situ* X-ray diffraction under autoclave condition

Jun Kikuma,^{a*} Masamichi Tsunashima,^a Tetsuji Ishikawa,^a Shin-ya Matsuno,^a Akihiro Ogawa,^b Kunio Matsui^b and Masugu Sato^c

^aAnalysis and Simulation Center, Asahi-KASEI Corporation, Japan, ^bAsahi-KASEI Construction Materials Corporation, Japan, and ^cIndustrial Application Division, SPring-8/JASRI, Japan.
E-mail: kikuma.jb@om.asahi-kasei.co.jp

Hydrothermal formation of tobermorite from a pre-cured cake has been investigated by transmission X-ray diffraction (XRD) using high-energy X-rays from a synchrotron radiation source in combination with a newly designed autoclave cell. The autoclave cell has a large and thin beryllium window for wide-angle X-ray diffraction; nevertheless, it withstands a steam pressure of more than 1.2 MPa, which enables *in situ* XRD measurements in a temperature range of 373 to 463 K under a saturated steam pressure. Formation and/or decomposition of several components has been successfully observed during 7.5 h of reaction time. From the intensity changes of the intermediate materials, namely non-crystalline C–S–H and hydroxyllellstadite, two pathways for tobermorite formation have been confirmed. Thus, the newly developed autoclave cell can be used for the analyses of reaction mechanisms under specific atmospheres and temperatures.

© 2009 International Union of Crystallography
Printed in Singapore – all rights reserved

Keywords: *in situ*; AAC; concrete; hydration; autoclave; high-energy X-rays.

1. Introduction

Autoclaved aerated concrete (AAC) is widely used as a building material because of its high heat-insulation efficiency and fire-resistance capability. Typically, the AAC is produced by hydrothermal treatment of quartz sand, lime, cement, gypsum, aluminium powder (as a gas-generation agent) and some other additives at high temperatures. Its predominant components are crystalline calcium silicate hydrates, such as tobermorite [$\text{Ca}_5\text{Si}_6\text{O}_{16}(\text{OH})_2 \cdot 4\text{H}_2\text{O}$].

Although the formation mechanism of such crystalline calcium silicate hydrates has been of great interest for decades, it has not been understood thoroughly owing to the difficulty in investigating under hydrothermal reaction atmosphere, *i.e.* an autoclave process.

One approach for investigating the formation processes is to analyze a series of X-ray diffraction (XRD) patterns from samples at different reaction stages (curing time or temperature), obtained by terminating the reaction in the middle of the autoclave process. However, such an *ex situ* approach includes ambiguity caused by temperature dependence of solubility, unfavourable reactions during the cooling process, variation among different pieces used as samples at different reaction stages, and so on.

Therefore *in situ* approaches are very effective for understanding the reaction in detail. There have been several *in situ* approaches for hydrothermal reactions by means of transmission XRD (Norby *et al.*, 1994; Christensen *et al.*, 2004; Jensen *et al.*, 2005; Jupe *et al.*, 2005, 2008; Norby, 2006, and references therein), transmission energy-dispersive XRD (O' Hare *et al.*, 1998; Shaw *et al.*, 2000; Colston *et al.*, 2005; Meller *et al.*, 2007; Norby, 2006, and references therein) and by neutron diffraction as well (Fehr *et al.*, 2003). In these XRD studies, synchrotron radiation has been utilized, taking advantage of its high

intensity and, more importantly, its high photon energy in order for the X-rays to penetrate samples of appropriate thickness. Most of the reaction cells used in these studies are quite small, like capillaries or thin pipes, because they make pressure sealing easier. However, the accuracy of the temperature and the pressure control in the cell would not be sufficient because it is difficult to attach sensors or valves directly to these kinds of cells. It is also difficult to set a sample and water (as a source of steam) separately using these cells, although it is important in AAC formation for the steam to be supplied constantly to the sample throughout the reaction.

In this study we have developed an autoclave cell for *in situ* transmission XRD to overcome these drawbacks, and successfully investigated the formation reaction of tobermorite.

2. Experimental

2.1. Materials and sample preparation

A mixture of 54.4 wt% crushed natural quartz sand, 4.7 wt% quicklime (Kawai Sekkai), 38.9 wt% high early strength Portland cement (HPC, Ube-Mitsubishi) and 2.0 wt% gypsum (Wako, research grade) was used as starting material. The chemical composition of the starting mixture is shown in Table 1. It was fully mixed in the presence of water at 323 K for several minutes using a motor-driven blade stirrer. The ratio of water to solid was set to be 0.75/1 by weight, and the molar ratio of calcium to silicon was adjusted to be 0.53/1, both of which are typical values for starting materials of AAC. We did not use any gas-generation agent because air bubbles may cause non-uniformity in the thickness of a small piece of sample. The mixture slurry was poured into a plastic beaker, sealed in a plastic bag, and

Table 1

Chemical composition of the starting mixture.

	Composition (wt%)
SiO ₂	60.2
CaO	30.5
Al ₂ O ₃	2.5
SO ₃	2.1
Fe ₂ O ₃	1.7
K ₂ O	0.4
MgO	0.4
Na ₂ O	0.1

kept at 333 K for more than 12 h to produce a pre-cured cake. The pre-cured cake was then cooled down and cut into a piece of size 6 mm × 18 mm and thickness 3.0 mm, just before *in situ* measurements were conducted.

2.2. Autoclave cell

A schematic of the newly developed autoclave cell is shown in Fig. 1. It is made of stainless steel and consists of a rectangular parallelepiped main body (capacity 35 ml) and a lid. Two beryllium windows (0.5 mm thick, 4 mm and 20 mm in diameter) are firmly welded onto the centre of each sidewall. It should be mentioned that beryllium has not been used for hydrothermal reaction cells in the literature, presumably owing to the risk of leakage, even though beryllium windows have great advantages such as low X-ray absorption and no interference signal in XRD patterns. The lower part of the cell is used as a water reservoir, typically filled with about 5 ml of distilled water. A sample piece is placed on top of the water reservoir using a mounting stand so that the sample is not in contact with the water directly.

Two thermocouples are inserted into the cell using Swagelok compression pipe fittings connected to the lid, one for monitoring the vapour temperature near the sample and the other for monitoring the water temperature. A digital pressure sensor is also connected to the lid in the same way for monitoring the pressure inside the cell. A diaphragm pump and a needle valve are connected to the branched line of the pressure sensor for the removal of the air inside.

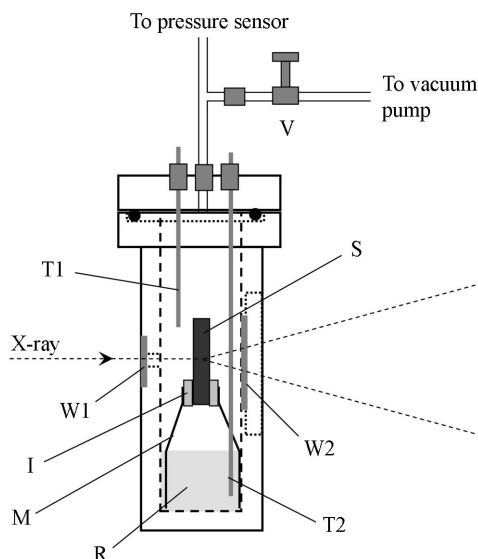


Figure 1

Schematic drawing of the autoclave cell for *in situ* transmission XRD. W1, W2: beryllium windows; R: water reservoir; T1, T2: thermocouples; M: sample mounting stand; I: heat insulators (Teflon pieces); V: needle valve; S: sample.

The main body and the lid are sealed by a heat-resistant rubber O-ring, and the cell reliably withstands pressures of at least 1.2 MPa at 473 K for more than 12 h.

The temperature of the cell is controlled by a copper heater block surrounded by a heat insulator.

2.3. *In situ* XRD measurement

In situ XRD measurements were carried out at the BL19B2 beamline of SPring-8, using an X-ray energy of 30 keV. The X-ray beam size was set to be 0.8 mm wide and 0.12 mm high. An imaging plate was placed downstream at a sample-to-detector distance of 726 mm.

The autoclave cell containing a sample and water was set in the copper heater block. First, the temperature was elevated to 373 K at a ramping rate of 2 K min⁻¹. The temperature was held at 373 K for 15 min. During this period the cell was evacuated for a few seconds, and about 95% of the air was removed from the cell. After the steam pressure built up again at 373 K, the first XRD measurement was conducted. After 15 min at 373 K, the temperature was elevated again to 463 K at a ramping rate of 1 K min⁻¹, then held at 463 K for 6 h. During this process the XRD measurements were conducted at intervals of either 15 or 30 min with an exposure time of 6 min. During the exposure time, the cell, together with the heater block, was oscillated in the vertical direction by 0.5 mm at a rate of 0.1 mm s⁻¹. The ring-shaped diffraction patterns were obtained for a 1/d range of 0.5–6.5 nm⁻¹, and their sector average was taken from -25° to 25°, and normalized with the transmitted beam intensities, to obtain one-dimensional diffraction patterns. These data analysis procedures were conducted by laboratory-made macro programs based on *IGOR Pro* software (Hulinks).

3. Results and discussion

Fig. 2 shows a series of XRD patterns in the vicinity of major tobermorite peaks. Most of the diffraction peaks are assigned to be those from major components, although there are some unidentified peaks presumably from minor components in cement and quartz sand, which contain natural materials. The intensities of the major peaks (peak area) are plotted in Fig. 3. For hydroxyllellastadite [HE; Ca₁₀(SiO₄)₃(SO₄)₃(OH)₂], the sum of three diffraction peak intensities, (211), (300) and (002), is plotted in order to obtain better statistics. The horizontal-axis values (time) of the data points are defined to be the time at which the exposure has started. The temperature and pressure inside the cell are shown at the top of Fig. 3. The steam temperature was measured a few millimetres away from the sample. Both the temperature and the pressure were very stable throughout the experiment.

At the beginning of the autoclave process (at 373 K), quartz, portlandite and monosulfate [MS; Ca₄Al₂O₆(SO₄)·12H₂O] were observed as major components. As the temperature increased, the MS peak diminished rapidly, indicating the dissolution of MS into an aqueous solution phase surrounding the solid phase (Christensen *et al.*, 2004). This should lead to an increase of SO₄ ion concentration in the solution phase. Then, HE began to be observed at 433 K. The fact that HE is formed right after the dissolution of MS indicates that the SO₄ ion from dissolved MS is used as a sulfur source for HE. Portlandite and quartz began to decrease after the temperature reached 463 K. Dissolved portlandite reacts with dissolved quartz to form non-crystalline calcium-silicate-hydrate (C-S-H). Non-crystalline C-S-H is also formed by hydration of cement, and is well known as a major intermediate material for tobermorite formation (Taylor,

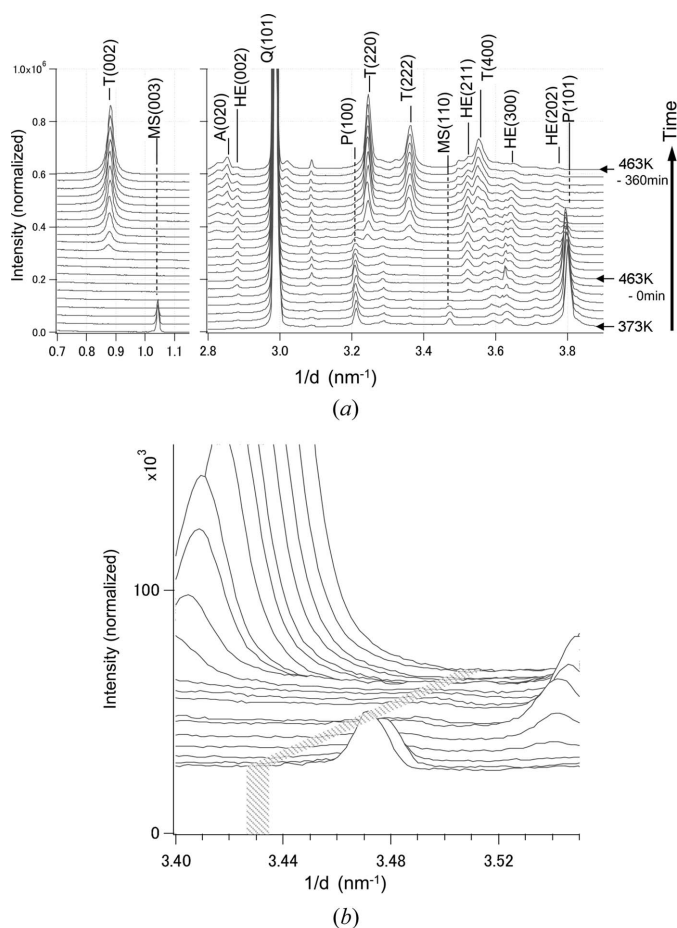


Figure 2

Stack of *in situ* XRD patterns obtained during the autoclave process. The reaction under the autoclave proceeds from bottom to top: the temperature was elevated from 373 K to 463 K and then held at 463 K for 6 h (see text). T: tobermorite; P: portlandite; Q: quartz; MS: monosulfate; HE: hydroxyllellastadite; A: anhydrite. (a) In the vicinity of major tobermorite peaks. (b) A close-up three-dimensional pattern in the vicinity of the C–S–H amorphous halo; the hatched area indicates the region by which the amount of C–S–H would be reflected.

1997). Then, tobermorite began to be observed at 60 min after the temperature reached 463 K, and kept increasing to the end of the curing time. Thus, the general formation process of tobermorite is well reproduced in the newly developed autoclave cell.

The advantage of an *in situ* experiment is the ability to investigate reaction pathways directly. Here, we would like to discuss two possible pathways of tobermorite formation observed in this study. The first is a formation *via* non-crystalline C–S–H. It should be mentioned that we were able to observe the intensity change of an amorphous halo around 3.4 nm⁻¹, where the halo of non-crystalline C–S–H is observed (Taylor, 1997). Generally, with an *ex situ* type of experiment, it is difficult to pursue the amount of non-crystalline materials during a reaction process because the intensity of the amorphous halo could be affected by the background intensity, which could vary among different pieces of the sample or by sample preparation. In an *in situ* experiment, however, the same portion of the sample is continuously measured throughout the experiment. This allows one to detect a slight change in amorphous intensity. A slight intensity change around 3.4 nm⁻¹ is shown in Fig. 2(b). The integrated intensity from 3.427 to 3.434 nm⁻¹ is plotted together in Fig. 3 (no background subtracted). The intensity increases with increasing temperature and reaches a maximum at around 150 min, which is the same timing as the drastic decrease of portlandite and the

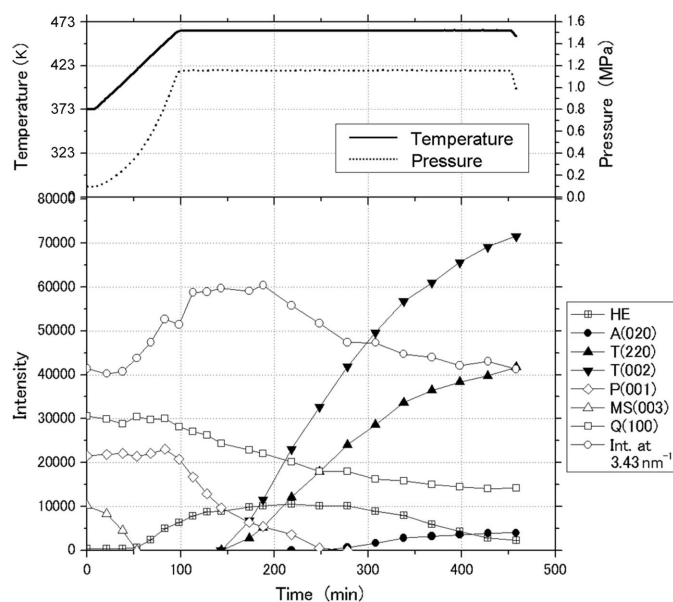


Figure 3

Top: time dependence of the temperature and the pressure inside the cell during the autoclave process. Bottom: time dependence of the intensities of the major components during the autoclave process. The sum of the HE(211), HE(300) and HE(002) peak intensities is indicated as HE intensity. T: tobermorite; P: portlandite; Q: quartz; MS: monosulfate; HE: hydroxyllellastadite; A: anhydrite.

beginning of tobermorite formation. Then the intensity decreases as the formation of tobermorite proceeds. Judging from this intensity change behaviour, it is reasonable to regard this amorphous halo as that from non-crystalline C–S–H. Thus, Fig. 3 indicates tobermorite formation *via* non-crystalline C–S–H.

The second pathway is that with HE as a calcium source. HE intensity reaches a plateau at 170–270 min, and then starts to decrease after 300 min. At the point that HE started to decrease, anhydrite started to be observed. It has been reported that HE reacts with dissolved quartz to form tobermorite and anhydrite (Sakiyama *et al.*, 2000). Simultaneous observation of the decrease of HE and the increase of anhydrite is considered to be evidence of the occurrence of the tobermorite formation *via* HE.

From the results described above, it is reasonable to consider that two kinds of reaction pathways occur in the tobermorite formation. It should be pointed out that non-crystalline C–S–H starts to decrease much earlier than HE, suggesting a difference in reactivity between these two intermediate materials. Further *in situ* experiments, in which the amount of HE formation during the autoclave process is changed, are in progress, in order to investigate the effect of HE in more detail.

Thus, the newly developed autoclave cell, combined with high-energy transmission XRD, can be used for *in situ* analyses of hydrothermal reactions. Using a CCD or a photon-counting pixel array detector, it is possible to conduct much faster measurements, enabling the reaction kinetics to be discussed. The autoclave cell can also be applied to other kinds of reactions that require specific temperatures, pressures and atmospheres.

This study was performed with the approval of JASRI (proposal Nos. 2008A1778 and 2008A1905).

References

- Christensen, A. N., Jensen, T. R. & Hanson, J. C. (2004). *J. Solid State Chem.* **177**, 1944–1951.

- Colston, S. L., Barnes, P., Jupe, A. C., Jacques, S. D. M., Hall, C., Livesey, P., Dransfield, J., Meller, N. & Maitland, G. C. (2005). *Cem. Concr. Res.* **35**, 2223–2232.
- Fehr, K. T., Huber, M., Zuern, S. G. & Peters, E. (2003). *Proceedings of the 7th International Symposium on Hydrothermal Reactions*, Changchun, China, pp. 19–25.
- Jensen, T. R., Christensen, A. N. & Hanson, J. C. (2005). *Cem. Concr. Res.* **35**, 2300–2309.
- Jupe, A. C., Wilkinson, A. P., Luke, K. & Funkhouser, G. P. (2005). *Ind. Eng. Chem. Res.* **44**, 5579–5584.
- Jupe, A. C., Wilkinson, A. P., Luke, K. & Funkhouser, G. P. (2008). *Cem. Concr. Res.* **38**, 660–666.
- Meller, N., Hall, C., Kyritsis, K. & Giritat, G. (2007). *Cem. Concr. Res.* **37**, 823–833.
- Norby, P. (2006). *Curr. Opin. Colloid Interface Sci.* **11**, 118–125.
- Norby, P., Christensen, A. N. & Hanson, J. C. (1994). *Stud. Surf. Sci. Catal.* **84**, 179–186.
- O'Hare, D., Evans, J. S. O., Francis, R. J., Halasyamani, P. S., Norby, P. & Hanson, J. (1998). *Microporous Mesoporous Mater.* **21**, 253–262.
- Sakiyama, M., Oshio, Y. & Mitsuda, T. (2000). *J. Soc. Inorg. Mater. Jpn*, **7**, 685–691.
- Shaw, S., Clark, S. M. & Henderson, C. M. B. (2000). *Chem. Geol.* **167**, 129–140.
- Taylor, H. F. W. (1997). *Cement Chemistry*, 2nd ed. London: Thomas Telford.